

Laboratory Investigations and Theoretical Analysis of Axial Thrust Problem in High Rotational Speed Pumps

ANDRZEJ WILK

Institute of Power Engineering and Turbomachinery

Silesian University of Technology

PL-44-100 Gliwice, Konarskiego 18

POLAND

awilk@imiue.polsl.pl <http://www.imiue.polsl.pl>

Abstract. Theoretical analysis of the influence of the increase of the rotational speed of the rotodynamic pump on axial thrust is made in the paper. The algorithm of the designing of the axial thrust relieving system by means of the relieving holes and relieving blades is presented.

The calculation examples for pump working at low and high rotational speed are included. The conclusions concerning with both axial thrust relieving systems for high rotational speed are presented.

The laboratory tests of rotodynamic pump working at rotational speed 6000 rpm are presented. The purpose of the tests was to determine the pump operation characteristics and pressure distribution around the impeller.

Key words: pump, high rotational speed, axial thrust, open impeller, radial blades, pressure distribution

1 Introduction

The tendency is noticed to increase the rotational speed of the rotodynamic pumps. Increasing the rotational speed makes possible to decrease overall dimensions and mass of the pump. It lets to increase fields of using the rotodynamic pumps – to obtain high delivery head at low discharge. It has been possible to obtain such parameters using positive pumps so far.

At high delivery head, the axial thrust is very high for closed or semi-open centrifugal impeller [1].

The relieving holes, the relieving blades or balancing disc are often used to relieve the axial thrust. The analysis of relieving the axial thrust by means of relieving holes and relieving blades are made in the paper.

Using these methods is not satisfactory solution to the axial thrust problem, therefore using the double-open impeller was considered.

High resultant tensions act in the open impellers with blades of single curvature. Blades with variable thickness must be used.

Centrifugal force “straighten” and deform the blade. It causes increasing of the outer diameter of the impeller. It causes necessity of using big radial and axial gaps between the impeller blades and the casing walls. A big gap causes high rate of leakage flow in the pump.

The open impeller with rectilinear radial blades seems to be a solution to these problems.

The laboratory investigations of the high rotational speed pump with double-open impeller with radial blades are presented in the next parts of the paper.

The aim of the investigations was to determine the pressure distribution around the impeller. The results of the tests confirmed the thesis, that such design of the impeller reduces the problems concerned with the axial thrust.

2 Balancing the Axial Thrust by the Relieving Holes

In case of the pumps working at high rotational speed high delivery head per pump stage is obtained. Higher axial forces and higher leakage in inner seals of the pump are present in consequence of it.

At high rotational speed balancing (relieving) the axial thrust is important in conjunction of bearing system durability.

Therefore designing of the axial thrust system needs particular care in such cases.

One of the method of relieving or balancing the axial thrust acting on closed, single-flow impeller of the pump is using the relieving holes. This method is common in one- and multi-stage pumps.

Relieving holes are made in rear impellers disc near the hub and there is the sealing behind the impeller. The sealing limits fluid flow through the holes. In such way the balancing chamber come into

existence. Because of connecting the balancing chamber with the suction side (inlet to the impeller) the pressure decreases in the balancing chamber.

Calculating respectively the diameter of the sealing behind the impeller it makes relieving, balancing or even changing the direction of the axial thrust possible.

When we use the relieving holes, the leakage (volumetric loses) arises in the sealing behind the impeller and leakage in sealing between the pump stages increases (in comparison with pump with ought relieving holes).

The volumetric loses causes decreasing of the pump discharge and should be considered at main impeller dimensions calculations.

So designing the balancing system lies in calculating the dimensions (mainly diameter of the sealing behind the impeller) what makes balancing the axial thrust components acting on the impeller and calculating of the rate of leakage flow possible.

2.1 The algorithm of the calculations of the axial thrust acting on the impeller and rate of leakage flow for axial thrust relieving system by the relieving holes

During defining the pressures acting on outside surfaces of the impeller it was supposed, that in the spaces in front of- and behind the impeller the liquid is rotating with the angular velocity proportional to the angular velocity of the impeller [2]. In such conditions the parabolic pressure distribution exists in this spaces (fig. 1). The way of the calculations concerned with designing of the relieving system is given below. One-dimension theory of flow through pump stage was used [3-6].

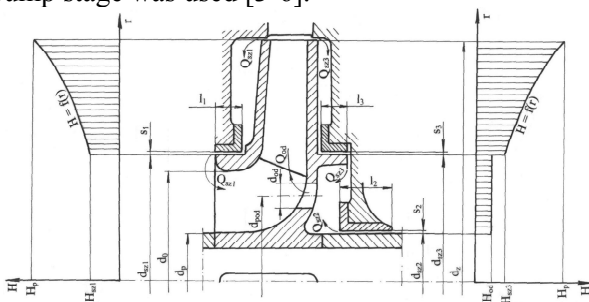


Fig. 1. Schema of the pump stage with the relieving holes

Static pressure head at the outlet of the pump impeller at nominal pump parameters

$$H_p = \Delta H \frac{\eta_{hw}}{\eta_h} \left(1 - \frac{g \cdot \Delta H}{2 \cdot \eta_h \cdot u_2^2} \right) \quad (1)$$

Hydraulic efficiency of the impeller

$$\eta_{hw} = \frac{1 + \eta_h}{2} \quad (2)$$

Velocity of transportation at the outlet of the impeller

$$u_2 = \frac{\Pi d_2 n}{60} \quad (3)$$

Static pressure head in front of the sealing slot at the inlet of the impeller

$$H_{sz1} = H_p - \frac{\omega^2 k_1^2}{2g} \left[\left(\frac{d_2}{2} \right)^2 - \left(\frac{d_{sz1}}{2} \right)^2 \right] \quad (4)$$

Angular velocity of the impeller

$$\omega = \frac{\Pi \cdot n}{30} \quad (5)$$

Rate of leakage flow in the sealing at the inlet to the impeller

$$Q_{sz1} = \frac{\Pi \cdot d_{sz1} \cdot s_{sz1} \sqrt{2gH_{sz1}}}{\sqrt{1 + \xi + \frac{2\lambda \cdot l_1}{s_{sz1}}}} \quad (6)$$

Velocity of the liquid at the inlet to the impeller

$$c_0 = \frac{4 \cdot (Q + Q_{sz1})}{\Pi \cdot (d_0^2 - d_p^2)} \quad (7)$$

Dynamic pressure head at the inlet the impeller

$$H_0 = \frac{c_0^2}{2 \cdot g} \quad (8)$$

Static pressure head in front of the sealing slot behind the impeller

$$H_{sz3} = H_p - \frac{\omega^2 k_2^2}{2g} \left[\left(\frac{d_2}{2} \right)^2 - \left(\frac{d_{sz3}}{2} \right)^2 \right] \quad (9)$$

Rate of leakage flow in the sealing behind the impeller

$$Q_{sz3} = \frac{\Pi \cdot d_{sz3} \cdot s_{sz3} \sqrt{2g(H_{sz3} - H_{od})}}{\sqrt{1 + \xi + \frac{2\lambda \cdot l_3}{s_{sz3}}}} \quad (10)$$

Rate of leakage flow in the sealing between pump stages

$$Q_{sz2} = \frac{\Pi \cdot d_{sz2} \cdot s_{sz2} \sqrt{2g(\Delta H - H_{od})}}{\sqrt{1 + \xi + \frac{2\lambda \cdot l_2}{s_{sz2}}}} \quad (11)$$

In case of the one-stage pumps or last pump stage of multi-stage pump $Q_{sz2} = 0$ [7].

Flow rate through the relieving holes

$$Q_{od} = \mu \cdot i_{od} \cdot \frac{\Pi d_{od}^2}{4} \sqrt{2g(H_{od} - H_o)} \quad (12)$$

Flow coefficient (number) through the relieving holes [8, 9]

$$\mu = 0,183 \cdot \ln \left(6\Pi \cdot \frac{v_o}{u_o} + 1 \right) \quad (13)$$

Liquid velocity in the relieving holes

$$v_o = \frac{4(Q_{od})}{\Pi \cdot i \cdot d_{od}^2} \quad (14)$$

Velocity of transportation of the relieving holes

$$u_o = \frac{\Pi \cdot d_{pod} \cdot n}{60} \quad (15)$$

Rate of leakage flow behind the impeller and flow rate through the relieving holes are connected with the relation

$$Q_{od} = Q_{sz2} + Q_{sz3} \quad (16)$$

It is possible to calculate pressure head in the balancing chamber H_{od} using formulas given above.

Axial force acting on the front impeller disc

$$F_1 = \Pi \cdot g \cdot \rho \cdot \left[\left(\frac{d_2}{2} \right)^2 - \left(\frac{d_{sz1}}{2} \right)^2 \right] \cdot \left\{ H_p - \frac{\omega^2 k_1^2}{4g} \left[\left(\frac{d_2}{2} \right)^2 - \left(\frac{d_{sz1}}{2} \right)^2 \right] \right\} \quad (17)$$

Axial force acting on the rear impeller disc outside the balancing chamber

$$F_2 = \Pi \cdot g \cdot \rho \cdot \left[\left(\frac{d_2}{2} \right)^2 - \left(\frac{d_{sz3}}{2} \right)^2 \right] \cdot \left\{ H_p - \frac{\omega^2 k_2^2}{4g} \left[\left(\frac{d_2}{2} \right)^2 - \left(\frac{d_{sz3}}{2} \right)^2 \right] \right\} \quad (18)$$

Axial force acting in the balancing chamber

$$F_3 = \Pi \cdot g \cdot \rho \cdot \left[\left(\frac{d_{sz3}}{2} \right)^2 - \left(\frac{d_{sz2}}{2} \right)^2 \right] \cdot H_{od} \quad (19)$$

Hydrodynamic reaction of the fluid flowing into the impeller

$$F_s = \rho \cdot c_0 \cdot (Q + Q_{sz1}) \quad (20)$$

Hydrodynamic reaction of the fluid flowing out of the relieving holes

$$F_{sod} = \rho \cdot v_0 \cdot (Q_{sz2} + Q_{sz3}) \quad (21)$$

Resultant axial force acting on the impeller

$$F = F_2 + F_3 - F_1 - F_s - F_{sod} \quad (22)$$

For balancing the axial thrust (in one impeller limits) such diameter of the sealing slot behind the impeller d_{sz3} should be calculated, that $F = 0$.

Fulfilment of the condition is possible only at nominal pump parameters. Laboratory investigations [10] have shown, that during decreasing of the pump discharge, the axial thrust increases. Axial thrust has maximum for discharges nearly equal or equal zero (investigations was made for pump with $d_{sz1} = d_{sz3}$). Increasing of the delivery head of the pump and increasing of the static pressure at the impeller outlet and changes in pressure distributions around the impeller causes the increase of the axial thrust.

Assuming, that angular velocity of the fluid in space in the impeller is equal angular speed of the impeller, it is possible to estimate the maximum static pressure at the outlet of the impeller from the formula

$$H_{p \max} = \frac{\omega^2}{2 \cdot g} \left[\left(\frac{d_2}{2} \right)^2 - \left(\frac{d_1}{2} \right)^2 \right] \quad (23)$$

Using pressure head calculated in such way it is possible to estimate the axial thrust at discharge equal zero (impeller discharge is equal rate of leakage flow in such conditions).

2.2 Calculating example for relieving the axial thrust by the relieving holes

Using the formulas given above the calculations were made for follow pump impellers:

A. multi-stage pump for rotational speed $n = 1450$ rpm, (not last stage)

B. one-stage pump for rotational speed $n = 1450$ rpm,

C. one-stage pump for rotational speed $n = 11800$ rpm,

Performance parameters of the analysed pumps are given in table 1, and basic design dimensions in table 2.

Table 1. Performance parameters of the analysed pumps

Parameter	Pump	A	B	C
discharge Q	m ³ /s	0,0225	0,0225	0,0025
delivery head for one pump stage ΔH	m	29	29	500
rotational speed n	rpm	1450	1450	11800
pumps hydraulic efficiency η_h	-	0,887	0,887	0,710

Table 2. Basic design dimensions of the analysed pumps

dimension	pump	A	B	C
d_2	m	0,300	0,300	0,168
d_0	m	0,122	0,122	0,032
d_p	m	0,0546	0,0546	0,000
d_{od}	m	0,015	0,015	0,005
i_{od}		6	6	10

It was assumed [2 – 5, 11, 13], that:

- proportional coefficients $k_1 = k_2 = 0,5$;
- local hydraulic loss factor $\xi = 0,5$

- linear hydraulic loss factor $\lambda = 0,01$.

The values of the axial thrust for impeller without the relieving holes were calculated. The axial thrust is respectively:

$$F_A = F_B = 1749 \text{ N} \quad F_C = 2490 \text{ N}$$

The diameter of the sealing d_{sz3} in purpose of complete balancing ($F = 0$) the axial thrust was calculated. Results are given in table 3.

Table 3. Parameters in pump stage for complete balancing ($F = 0$) the axial thrust

Parameter	pump	A	B	C
H_p	m	21,31	21,31	409,07
H_{sz1}	m	16,03	16,03	285,97
H_{sz3}	m	16,10	16,08	286,61
H_{od}	m	1,40	1,14	28,37
Q_{sz1}	m ³ /s	0,000881	0,000881	0,001492
Q_{sz2}	m ³ /s	0,000353	0	0
Q_{sz3}	m ³ /s	0,000864	0,000866	0,001450
Q_{ot}/Q		0,0541	0,0385	0,58
μ		0,249	0,206	0,322
F	N	0	0	0

Next, for calculated diameter of the balancing chamber sealing, the axial thrust for $Q = 0$ was calculated (at maximum delivery head of the impeller) Results are given v table 4.

Table 4. The parameters in pump stage at zero discharge

parameter	pump	A	B	C
$H_{p \max}$	m	22,21	22,21	509,74
H_{sz1}	m	16,93	16,93	386,64
H_{sz3}	m	17,00	16,98	387,28
H_{od}	m	1,47	1,15	33,52
d_{sz3}	m	0,1379	0,1370	0,0552
Q_{sz1}	m ³ /s	0,000905	0,000905	0,001735
Q_{sz2}	m ³ /s	0,000306	0	0
Q_{sz3}	m ³ /s	0,000888	0,000891	0,001697
Q_{ot}/Q		0,0531	0,0396	0,68
μ		0,247	0,209	0,346
F	N	0	0	-54

2.3 Conclusions concerned with using the relieving holes in high rotational speed pumps

By analysing the results of the calculations related to balancing the axial thrust by the relieving holes, ones can come to the conclusions:

- the axial thrust for impellers without relieving holes has considerable value, therefore the axial thrust should be relieved (balanced),

- in case of using the relieving holes it is possible to balance the axial thrust (in case of one- and multi-stage pumps),
- in case of using the relieving holes it is possible to balance the axial thrust either in case of pump working with low or high rotational speeds.
- it is necessary to assure low pressure in balancing chamber proper work of the balancing system. It is possible to obtain such conditions by good sealing of the balancing chamber,
- the width of the gap s_1 has essential meaning for rate of leakage flow [14]. Considerable rate of leakage flow in the one-gap sealing at impeller inlet occurs in case of the high rotational speed pumps

Decreasing of the gap width s is limited by technological purposes. Therefore flow rate through the relieving holes and sealing at the impeller inlet increases together with pump rotational speed.

Using the sealing gap in the axial thrust balancing systems with relieving holes in high rotational speed pumps causes significant decreasing the pump efficiency.

3 Balancing the Axial Thrust by the Relieving Ribs

Another method of the relieving the axial thrust is using the relieving ribs. Relieving ribs are placed on the impeller rear disc. The liquid in the space behind the impeller rotates with the higher rotational speed then in case of the disc without the ribs. It causes change of the pressure distribution and relieving the axial thrust (Fig. 2).

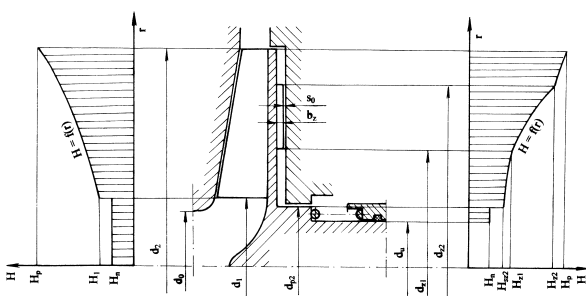


Fig. 2. Schema of the pump stage with the relieving ribs

Calculating respectively the dimensions of the relieving ribs it makes relieving, balancing or even changing the direction of the axial thrust possible.

The essential task in designing the balancing system with the relieving ribs is calculating the dimensions of the relieving ribs what makes decreasing resultant axial thrust.

3.1 The algorithm of the calculations of the axial thrust for semi-open impeller with the relieving ribs

The calculations we made for the closed impeller have shown, that in case of the closed impellers working at high rotational speed there is the significant pressure difference in the sealing at the impeller inlet. For the technological and exploitations reasons it is not possible to decrease the width of this gap infinitively or use two-gap seals. Therefore the rate of leakage flow between space in front of the impeller and inlet to the impeller is significant and causes decreasing the volumetric efficiency of the pump. Impeller without the front disc (semi-open impeller) has no such disadvantage. Therefore below given algorithm of designing the axial thrust balancing system is given for semi-open impeller. One-dimension theory of flow through pump stage was used [3 - 6].

Rotodynamic pumps for high rotational speed often needs affluence for proper work. Therefore the axial force connected with the affluence pressure was considered in the calculations

Hydraulic efficiency of the impeller

$$\eta_{hw} = \frac{1 + \eta_h}{2} \tag{24}$$

Angular velocity of the impeller

$$\omega = \frac{\Pi n}{30} \tag{25}$$

Velocity of transportation at the outlet of the impeller

$$u_2 = \frac{d_2 \omega}{2} \tag{26}$$

Static pressure head at the outlet of the pump impeller at nominal pump parameters

$$H_p = \Delta H \frac{\eta_{hw}}{\eta_h} \left(1 - \frac{g \cdot \Delta H}{2 \cdot \eta_h \cdot u_2^2} \right) \tag{27}$$

Assuming the parabolic pressure distribution in the space around the impeller it is possible to calculate the coefficient of the rotational speed of the liquid

$$k_1 = \sqrt{\frac{2gH_p}{\omega^2 \left[\left(\frac{d_2}{2} \right)^2 - \left(\frac{d_1}{2} \right)^2 \right]}} \tag{28}$$

Axial force acting in the semi-open impellers surface

$$F_1 = \Pi \cdot g \cdot \rho \cdot \left[\left(\frac{d_2}{2} \right)^2 - \left(\frac{d_1}{2} \right)^2 \right] \cdot \left\{ H_p - \frac{\omega^2 k_1^2}{4g} \left[\left(\frac{d_2}{2} \right)^2 - \left(\frac{d_1}{2} \right)^2 \right] \right\} \quad (29)$$

Velocity of the liquid at the inlet to the impeller

$$c_0 = \frac{4 \cdot Q}{\Pi \cdot d_0^2} \quad (30)$$

Hydrodynamic reaction of the liquid flowing into the impeller

$$F_s = \rho \cdot c_0 \cdot Q \quad (31)$$

Axial force induced by affluence pressure

$$F_n = \Pi \cdot g \cdot \rho \cdot \left(\frac{d_u}{2} \right) \cdot H_n \quad (32)$$

Axial force acting on the impellers rear disc surface without the ribs

$$F_3 = \Pi \cdot g \cdot \rho \cdot \left[\left(\frac{d_2}{2} \right)^2 - \left(\frac{d_{z2}}{2} \right)^2 \right] \cdot \left\{ H_p - \frac{\omega^2 k_3^2}{4g} \left[\left(\frac{d_2}{2} \right)^2 - \left(\frac{d_{z2}}{2} \right)^2 \right] \right\} \quad (33)$$

Pressure head at the outer diameter of the relieving ribs

$$H_{dz2} = H_p - \frac{\omega^2 k_3^2}{2g} \left[\left(\frac{d_2}{2} \right)^2 - \left(\frac{d_{z2}}{2} \right)^2 \right] \quad (34)$$

Coefficient of the rotational speed of the liquid behind the impeller

$$k_4 = 0,5 \left(1 + \frac{b_z}{b_z + s_0} \right) \quad (35)$$

Axial force acting on the impellers rear disc surface with the ribs

$$F_4 = \Pi \cdot g \cdot \rho \cdot \left[\left(\frac{d_{z2}}{2} \right)^2 - \left(\frac{d_{z1}}{2} \right)^2 \right] \cdot \left\{ H_{dz2} - \frac{\omega^2 k_4^2}{4g} \left[\left(\frac{d_{z2}}{2} \right)^2 - \left(\frac{d_{z1}}{2} \right)^2 \right] \right\} \quad (36)$$

Pressure head at the inner diameter of the relieving ribs

$$H_{z2} = H_{dz2} - \frac{\omega^2 k_4^2}{2g} \left[\left(\frac{d_{z2}}{2} \right)^2 - \left(\frac{d_{z1}}{2} \right)^2 \right] \quad (37)$$

Axial force acting on the impeller's rear disc surface without the ribs

$$F_5 = \Pi \cdot g \cdot \rho \cdot \left[\left(\frac{d_{z1}}{2} \right)^2 - \left(\frac{d_{p2}}{2} \right)^2 \right] \cdot \left\{ H_{dz1} - \frac{\omega^2 k_5^2}{4g} \left[\left(\frac{d_{z1}}{2} \right)^2 - \left(\frac{d_{p2}}{2} \right)^2 \right] \right\} \quad (38)$$

Pressure head at the inlet to the sealing gap

$$H_{sz2} = H_{dz1} - \frac{\omega^2 k_5^2}{2g} \left[\left(\frac{d_{z1}}{2} \right)^2 - \left(\frac{d_{p2}}{2} \right)^2 \right] \quad (39)$$

Resultant axial force acting on the impeller

$$F = F_3 + F_4 + F_5 - F_1 - F_s - F_n \quad (40)$$

Positive value of the axial thrust means it is directed to the suction side of the pump, negative value – to the pressure side.

3.2 Calculating example for relieving the axial thrust by the relieving ribs

Using the formulas given above the calculations were made for the stage of the high rotation speed pump. Performance parameters are as it follows:

- discharge $Q = 0,0025 \text{ m}^3/\text{s}$
- delivery head per one stage $\Delta H = 500 \text{ m}$
- rotational speed $n = 11800 \text{ rpm}$
- hydraulic effectiveness of the pump $\eta_h = 0,710$

The pump has main dimensions as it follows:

- diameter if the impeller's blade beginning $d_1 = 0,045 \text{ m}$
- outer diameter of the impeller $d_2 = 0,168 \text{ m}$

- diameter of the impeller's inlet $d_0 = 0,032$ m
- width of the relieving rib $b_z = 0,003$ m
- width of the gap behind the impeller $s_0 = 0,0002$ m

The proportional coefficients for the spaces without the ribs were assumed [2 – 5, 11, 13] $k_3 = k_5 = 0,5$.

Pressure head of the affluence $H_n = 100$ m

3.2.1 Calculations at pump nominal parameters

The proportional coefficients (of the fluid rotation) in the space with the ribs k_4 depend on the width of the gap s_0 between the ribs and pump casing. When width of the gap increases (caused for example by erosion of the casing or improper assemblage of the pump) the pressure distribution and axial thrust changes. The calculation results for nominal pump parameters for different width of the gap ($s_0 = 0,004 \div 0,0015$ m) are given in the table 5.

Table 5. Axial thrust for the nominal pump parameters for different width of the gap s_0

s_0	mm	0,4	0,6	0,8	1,0	1,2	1,4
H_p	m	409,07					
H_{dz2}	m	409,07					
H_1	m	0					
H_{dz1}	m	-19,38	2,64	21,86	38,75	53,71	67,04
H_{sz2}	m	-22,08	-0,06	19,16	36,05	51,01	64,34
F_1	N	41287					
F_s	N	8					
F_n	N	1775					
F_3	N	0					
k_4		0,941	0,917	0,895	0,875	0,857	0,841
F_4	N	37321	39430	41270	42888	44321	45598
F_5	N	-89	6	88	160	224	281
F	N	-5838	-3635	-1712	-22	1475	2809

It can be concluded, that the axial thrust increases together with the width of the gap s_0 . Relation between axial thrust and the width of the gap is shown in the fig. 3.

3.2.2 Calculations for the different delivery head of the pump

When the discharge of the pump changes, also delivery head of the pump and static pressure head H_p at the impeller outlet changes.

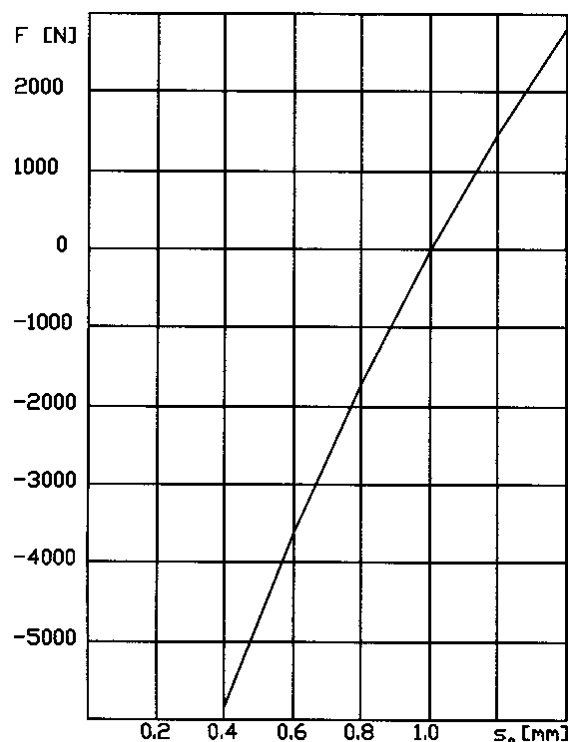


Fig. 3. Relieving the axial thrust with the relieving ribs. Relation between axial thrust F and the width of the gap s_0 for the nominal pump parameters.

Pressure changes in the spaces around the impellers cause changes of the axial thrust. It is possible to define pressure changes using theoretic analyses, laboratory tests or numerical modelling [3 – 6, 12, 16 - 19]. The results of the calculations for different delivery head (for constant gap width $s_0 = 0,0010$ m) are given in the table 6.

Table 6. Axial thrust for different delivery head for constant gap width $s_0 = 0,0010$ m

H_p	m	510	475	450	400	300	200
k_1		1,000	0,965	0,940	0,886	0,767	0,626
H_1	m	0					
H_{dz1}	m	139,7	104,7	79,7	29,7	-70,3	-170,3
H_{sz2}	m	137,0	102,0	77,0	27,0	-73,0	-173,0
F_1	N	51473	47941	45418	40371	30279	20186
F_s	N	8					
F_n	N	1775					
F_3	N	0					
F_4	N	62220	55516	50727	41150	21996	2842
F_5	N	592	442	335	121	-306	-734
F	N	9555	6234	3862	-883	-10372	-19860

It can be concluded, that axial thrust increases together with the delivery head. The relation between axial thrust F and the static pressure head at the impeller outlet H_p is given in fig. 4.

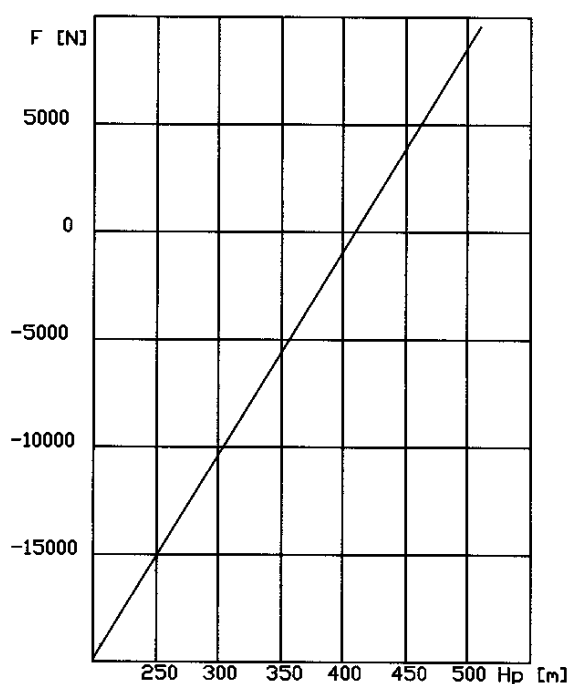


Fig. 4. Relieving the axial thrust with the relieving ribs. The relation between axial thrust F and the static pressure head at the impeller outlet H_p for constant gap width $s_0 = 0,0010$ m

3.3 Conclusions concerned with using the relieving ribs in high rotational speed pumps

By analysing the results of the calculations related to balancing the axial thrust by the relieving ribs in high rotational speed pumps, ones can come to the conclusions:

- axial thrust components have considerable values,
- in case of using the relieving ribs it is possible to balance the axial thrust only for selected operational point (selected parameters). It is not possible to balance axial thrust in the whole range of the parameters,
- changes of the width of the gap between the edge of the relieving ribs and the pump casing causes considerable changes of the axial thrust,
- at performance parameters different than nominal, the axial thrust may have considerable values.

In case of high rotational speed pumps both the change of the performance parameters and the change of the width of the gap between relieving ribs and pump casing causes change of the axial

thrust. Big values of the axial thrust may lead to significant decrease of durability of the pump bearing system. In extremely disadvantageous combination of work conditions quick destruction of bearings may occur.

4 Laboratory Tests of the Pump with Double-Open Impeller

4.1 Aim of the tests

It may be predicted, that in case of double-open impeller using, pressure distribution around the impeller (in front of- and behind the impeller) should be similar at whole range of discharge. In such case the axial thrust will be small and its relieving - simple. To verify the thesis, the laboratory tests of the pump with double-open impeller were made. The aim of the tests was to determine pressure distribution around the impeller of the pump at rotation speed $n_{nom} = 6000$ rpm.

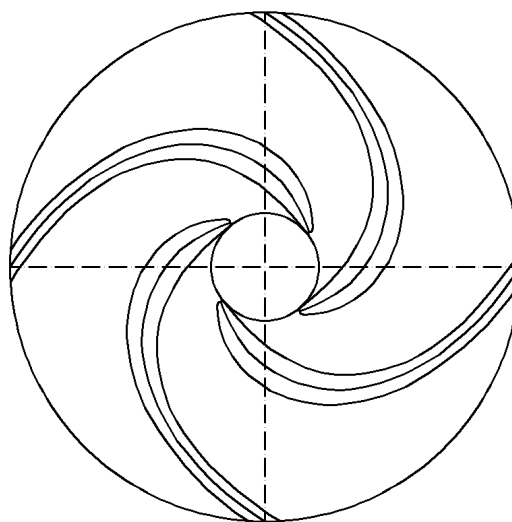


Fig. 5. The impeller with constant strength blades



Fig. 6. View of the constant strength blade deformed by centrifugal force

High resultant tensions act in the blade in the double-open impeller with blades of single curvature. It is not possible to use blades with constant thickness. Blades with variable thickness (constant strength) have to be used. The impeller with constant strength of high-speed pump is presented in fig. 5.

But tensions acting in a blade with single curvature cause deformations of the blade. Centrifugal force “straighten” and deform the blade. It causes increase of the outer diameter of the impeller. It causes necessity of using big radial and axial gaps between the impeller blades and the casing walls. A big gap causes high volumetric loses in the pump.

In the fig. 6. the view of the blade designed as blade with constant strength is presented. During work at rotation speed $n = 11800$ rpm centrifugal force acting on the impeller causes crossing the plastic range of the blade material and its deformation, increasing impeller diameter and its destruction.

The open impeller with rectilinear radial blades seems to be a solution to these problems.

4.2 Description of the model pump

Laboratory tests discussed in this paper were carried out on model pump specially designed for these tests.

Main (centrifugal) impeller has rectilinear radial blades. For the constructional (bind the blades to the hub) and strength reasons the impeller has residual back disk. Centrifugal impeller is presented in Fig. 8.

It is a one-stage pump with initial impeller. The pump has a horizontal axis.

Initial impeller is shaped like one twist worm screw with constant inner diameter and constant outer diameter. Initial impeller is presented in Fig. 7.



Fig. 7. The initial impeller



Fig. 8. The centrifugal impeller

The pump has mechanical sealing. The pump shaft has its own ball bearings.

The pump has spiral casing [18].

It is possible to carry out the laboratory tests at the rotation speed up to 12000 rpm.

It is possible to carry out the tests for initial impellers with different pitch of the screw line and centrifugal impellers with different outer diameters, different diameters of blade beginning, different width of the blades and different gaps between impeller and casing.

The model pump is presented in Fig. 9.



Fig. 9. The model pump

5 Laboratorial Tests

Laboratory tests were carried out at rotation speed $n_{nom} = 6000$ rpm.

During the tests following impellers were used:

Initial impeller:

- outer diameter of the impeller $d_{s2} = 0.040$ m,
- hub diameter $d_{s1} = 0,015$
- pitch of the screw line $t_s = 0,021$ m
- number of pitches of the screw line $z_s = 2$

- width of the radial gap between the outer diameter of the initial impeller and the casing $s_s = 0,001$ m

Centrifugal impeller:

- outer diameter of the impeller $d_2 = 0,180$ m
- diameter of blades beginning $d_1 = 0,060$ m
- width of the blade at the inlet $b_1 = 0,018$ m
- width of the blade at the outlet $b_2 = 0,009$ m
- number of the blades $z = 12$.
- width of the axial gap between front wall of the casing and the blades of the impeller $s_1 = 0,003$ m
- width of the gap between back wall of the casing and the blades of the impeller $s_2 = 0,003$ m

Tests were made in accordance with Standard PN-EN ISO 5198:2002 (*Centrifugal, mixed flow and axial pumps - Code for hydraulic performance tests - Precision class*)

Laboratory tests were made in the Laboratory of Hydraulic Machines of the Institute of Power Engineering and Turbomachinery of the Silesian University of Technology, Gliwice, Poland.

The aim of the tests was to determine pump flow characteristics $H = f(Q)$ and $\eta = f(Q)$ at rotation speed $n_{nom} = 6000$ rpm

Additionally, the pressures were measured in space around the impeller i.e. pressure at the inlet to centrifugal impeller and pressures at the casing walls in front of the impeller and behind the impeller. Pressures were measured at different radiuses.

Delivery head was calculated as

$$H_m = \frac{p_2 - p_1}{\rho \cdot g} + \frac{w_2^2 - w_1^2}{2 \cdot g} + \Delta z \quad [m] \quad (41)$$

Pump efficiency was calculated as

$$\eta = \frac{Q_p \cdot H_m \cdot \rho \cdot g}{1000 \cdot P} \quad (42)$$

Rotation speed during measurements was not exactly equal to nominal so pump parameters were corrected as follows

$$Q = Q_p \cdot \left(\frac{n}{n_{nom}} \right) \quad (43)$$

$$H = H_m \cdot \left(\frac{n}{n_{nom}} \right)^2 \quad (44)$$

6 Tests Results

The test results are presented in graphs.

Pump characteristics are presented in fig. 10.

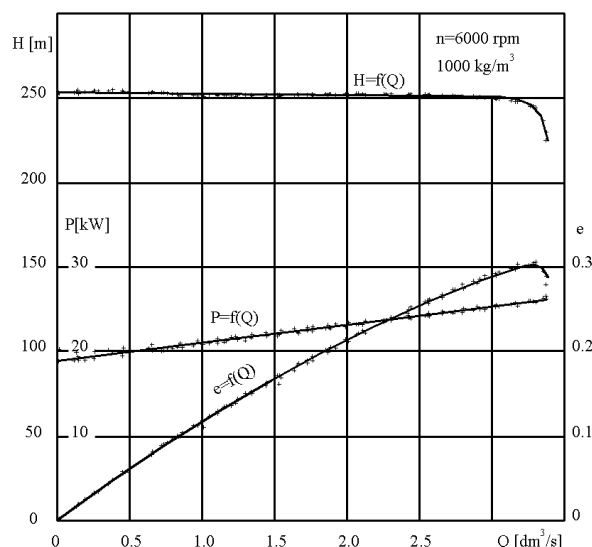


Fig. 10. Pump performance characteristics

Pressure head behind initial impeller in the function of discharge is presented in fig. 11.

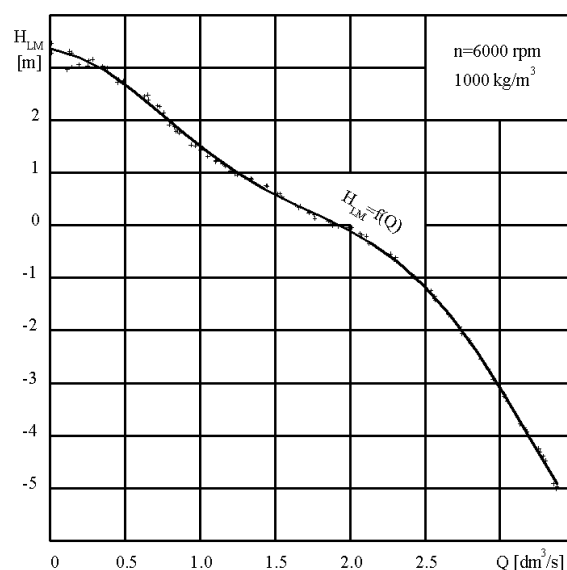


Fig. 11. Pressure head behind the initial impeller in the function of discharge

Fig. 12 presents pressure head in front of the impeller and behind it at different radiuses. Fig. 13 shows pressure head in front of and behind the impeller in the function of radius at discharge $Q = 1.45$ dm³/s.

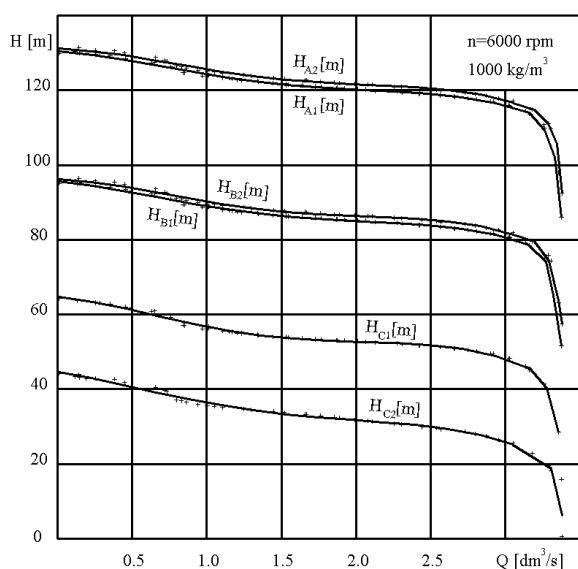


Fig. 12. Pressure head in front of the impeller and behind it at different radiuses

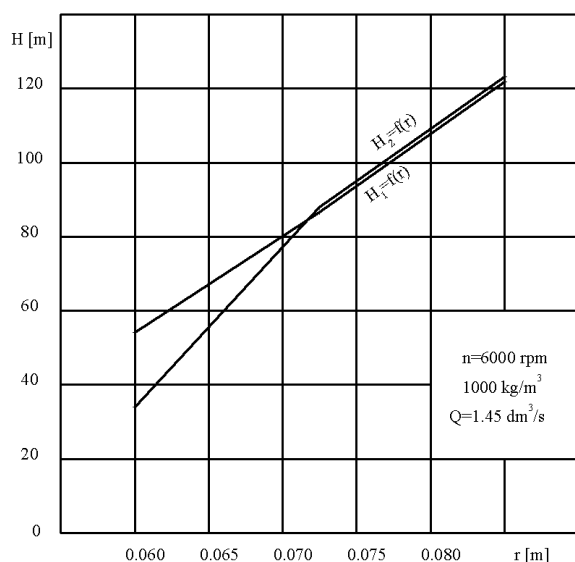


Fig. 13. Pressure head in front of and behind the impeller in the function of radius

7 Conclusions

1. Pump with tested initial impeller had not any higher discharge, because at discharge $Q > 2 \text{ dm}^3/\text{s}$ there was underpressure behind initial impeller (before centrifugal impeller) and at discharge $Q = 3.3 \text{ dm}^3/\text{s}$ there were cavitations in the pump. Initial impeller with higher pitch of the screw line should be used to obtain higher discharges.

In the tested range efficiency of the pump increases, what means that with such combination of impellers (initial and centrifugal) the pump did not reach nominal (optimal) parameters.

2. Head/discharge characteristic $H = f(Q)$ is nearly a straight horizontal line. For rotodynamic pumps with “classic” impellers delivery head decreases with increasing of the discharge.
3. Pressures in the spaces around the double-open impeller, in front of- and behind the impeller have similar values (at the same radiuses) in whole range of performance parameters. Resultant axial force as a result of pressure forces acting is not big.
4. Relation between pressure at wall before the impeller and radius is linear. Pressure at wall behind the impeller near the hub is little lower than at the same radius in front of the impeller. Ending of the impeller back disk probably causes it. Although the impeller is open, pressure distribution is not the same. It must be taken into consideration during axial thrust calculations.

Realised laboratory tests of the high rotational speed pump with double-open impeller with radial blades confirmed the thesis, that such solution is better with regards to axial thrust. The delivery head of the pump is high. Similar pressure distributions at both sides of the impeller caused, that resultant axial thrust is not big. It was confirmed by numerical calculations by CFD methods [19]. It is also advantageous, that pressure distribution is similar in whole range of pump performance parameters.

Acknowledgements

The author would like to thank the Polish Ministry of Science and High Education for the financial support of the research project no 4 T07B 012 30

Notation schedule

- b_z - width of relieving rib, m
- c - velocity, m/s
- d_0 - diameter of the inlet to impeller, m
- d_{od} - diameter of the relieving holes, m
- d_p - diameter of the impeller hub, m
- d_{pod} - dividing diameter of relieving holes, m
- d_{sz} - diameter of sealing gap, m
- d_2 - outer diameter of the impeller, m
- F - force, N
- g - acceleration of gravity, m/s^2
- H - total delivery head of the pump, m
- H_{A1}, H_{A2} - pressure head in front of/behind the impeller measured at radius $r_A = 0,085 \text{ m}$
- H_{B1}, H_{B2} - pressure head in front of/behind the impeller measured at radius $r_B = 0,0725 \text{ m}$
- H_{C1}, H_{C2} - pressure head in front of/behind the impeller measured at radius $r_C = 0,060 \text{ m}$

H_{dz} - pressure head at the end of relieving rib, m
 H_{LM} - delivery head of initial impeller, m
 H_m - total measured delivery head of the pump, m
 H_{sz} - pressure head at the inlet to the gap, m
 H_p - static delivery head at the impeller outlet, m
 ΔH - delivery head per one pump stage, m
 i_{od} - number of relieving holes,
 k - proportional coefficient,
 l - length of the sealing gap, m
 n - rotational speed, rpm
 n_{nom} - nominal rotational speed, rpm
 p_1 - pressure at pump inlet, Pa,
 p_2 - pressure at pump outlet, Pa,
 P - mechanical power, kW
 Q - volumetric flow rate, discharge, m^3/s
 Q_{od} - flow rate through the relieving holes, m^3/s
 Q_p - measured discharge, m^3/s
 Q_{sz} - flow rate through the gap, m^3/s
 s - width of the gap, m
 s_{sz} - width of the sealing gap, m
 u - velocity of transportation, peripheral velocity, m/s
 v - velocity, m/s
 v_o - velocity of flow through the relieving holes, m/s
 w_1 - velocity of liquid at pump inlet, m/s,
 w_2 - velocity of liquid at pump outlet, m/s
 Δz - geometrical pump height, m
 η - pump efficiency,
 η_h - hydraulic efficiency,
 η_{hw} - hydraulic efficiency of the impeller,
 λ - linear hydraulic loss factor,
 μ - coefficient (number) of flow through relieving holes,
 ξ - local hydraulic loss factor
 ρ - density of liquid, kg/m^3
 ω - angular velocity, 1/s

References

- [1] A. Wilk, Analiza odciążenia naporu osiowego za pomocą łopatek odciążających w pompach wirowych na duże prędkości obrotowe, *SYSTEMS Journal of Transdisciplinary Systems Science*, vol. 8/2003, ss. 520 – 527,
- [2] A. Wilk, S. Wilk, Testing of the effect which relieving radial blades have on power loss and pressure distribution, *PUMPENTAGUNG*, Karlsruhe 1996 r.
- [3] W. Jedral, *Pompy wirowe*, PWN Warszawa 2001 r.
- [4] A. Trokolanski, S. Lazarkiewicz, *Pompy wirowe*, WNT, Warszawa 1973 r.
- [5] J. Stepanoff, *Centrifugal and axial flow pumps*, John Wiley & Sons, Inc. Publishers, New York 1957 r.
- [6] T. Tanaka, Conservation Law of Centrifugal Force and Mechanism of Energy Transfer Caused in Turbomachinery, 4th WSEAS International Conference on Fluid Mechanics and Aerodynamics, Elounda, Greece 2006, pp. 337-342, (www.wseas.org/online)
- [7] S. Wilk, A. Wilk, Wpływ odciążenia na ciśnienie w dławnicach tłocznych pomp do cieczy zanieczyszczonych, *Maszyny Gornicze* nr 47/1994 r.
- [8] A. Wilk, Coefficient of Flow through the Holes in the Rotating Disc, 3rd ASME/JSME Joint Fluids Engineering Conference, San Francisco, USA 1999 r., Proceedings of the conference on CD-ROM no. FEDSM99-7343
- [9] A. Wilk, Współczynnik przepływu przez otwory odciążające w wirniku pompy wirowej, *Rozprawa doktorska*, Wydział Inżynierii Środowiska i Energetyki Politechniki Śląskiej w Gliwicach, 1998 r.
- [10] J. Debiec, Zrownowazenie naporu osiowego wirnika pompy odsrodkowej za pomocą otworów odciążających, *Zeszyty Naukowe Politechniki Śląskiej, Seria Energetyka*, zeszyt 61, Gliwice 1977 r.
- [11] W. Jedral, Metoda obliczania sił wzdłużnych w pompach wirowych, *Przegląd Mechaniczny* 13/1992
- [12] S. Wilk, *Gornicze pompy wirowe*, Śląskie Wydawnictwo Techniczne, Katowice, 1994 r.
- [13] A. Wilk, Badania rozkładu ciśnienia i straty mocy tarczy wirującej w obudowie o uzebrowanej ścianie, XI Konferencja Naukowa Problemy Rozwoju Maszyn Roboczych, Zakopane 1998 r.
- [14] S. Wilk, A. Wilk, Badania wpływu szczeliny w uszczelnieniu wirnika na wlocie na parametry pracy pompy do hydrotransportu, *Maszyny Gornicze* nr 50/1994 r.
- [15] N. Vlachakis and A. Baldoukas, On the centrifugal pumps performance curves estimation using empirical equations, WSEAS International Conference Information Science and Applications '02 (2nd ISA), Cancun, Mexico 2002, pp. 2941 – 2943, (www.wseas.org/online)

- [16] N. Krause, E. Pap, D. Thevenin, Part-load flow instabilities in a radial pump measured with TR-PIV, 4th WSEAS International Conference on Fluid Mechanics and Aerodynamics, Elounda, Greece, 2006, pp 319 – 324, (www.wseas.org/online)
- [17] V. Grapsas, J. Anagnostopoulos, D. Papantonis, Experimental and numerical study of a radial flow pump impeller with 2D-curved blades, 5th IASME / WSEAS International Conference on Fluid Mechanics and Aerodynamics, Athens, Greece, 2007, pp. 175 – 180, (www.wseas.org/online)
- [18] A. Wilk, Analiza wpływu zmniejszenia średnicy zewnętrznej wirnika na parametry pracy pompy wirowej ze spiralnym kanałem zbiorczym projektowanym metodą stałego kretu, V Konferencja Naukowo-Techniczna Racjonalizacja Gospodarki Energetycznej REGOS'2007, ss. 297 – 304, Łódź 2007
- [19] S. Dykas, A. Wilk, Determination of the flow characteristic of the high-rotational centrifugal pump by means of CFD methods, Tasc Quarterly, vol. 12, No 3-4/2008 , pp.245 – 255